Iranian Journal of Astronomy and Astrophysics
Vol. 11, No. 2, Spring 2024, 155–167
©Available online at http://ijaa.du.ac.ir
DOI: 10.22128/ijaa.2024.834.1184
Online ISSN: 2383–403X

Iranian Journal of Astronomy and Astrophysics

Research Paper

Variable Mass of the Test Particle in the Collinear 4-Body System with Triaxial Primaries

Abdullah[1] · Rabah Kellil*[2]
[1] Dyal Singh College, University of Delhi, Delhi, India;
email: abdullah@dsc.du.ac.in; abdullah2008@rediffmail.com
[2] Laghrour Abbes University, Khenchela, Algeria;
*email: kellilrabah@yahoo.fr

Received: 27 May 2024; Accepted: 25 November 2024; Published: 2 December 2024

Abstract. The mass variation effect of the test particle is studied in the collinear restricted four-body configuration with the assumption that the shapes of the three primary bodies are triaxial. It is assumed that these three primary bodies are placed in consecutive order on the abscissa axis and their axes are always parallel to the synodic ones. We also consider that the central body have solar radiation effect and the whole system is affected by Coriolis as well as centrifugal forces. Under these assumptions and using Jeans' law, the equations of motion and quasi-Jacobian integral are determined. And hence, the locations of parking points, Poincaré surfaces of section, surfaces with projection and basins of attractions are illustrated for the various values of the variation parameters. Furthermore, the stability of the parking points are examined in the in-plane as well as in the out-of-plane.

Keywords: Mass variation effect, Triaxial bodies, Parking points, Projections

1 Introduction

Since the dawn of time, man has always sought to know the secrets of the universe that surrounds him and also the laws that govern the motion of the stars and thus, he was getting ale to predict the future positions of the stars and planets. Among other questions he asked, was whether the celestial bodies have free behaviors or interact with each other. With Newtonś laws, this last question was solved, however, these laws only implicitly describe the motion of each of the components of a stellar system. Consequently, the various researchers were interested in solving the equations of motion of each of the components of a stellar system under different possible configurations ranging from the geometry of their locations to that of their forms, the radiation they emit, the forces they generate, their number, the possible variations in the mass of a part or all of these components, etc. Then these problems took which we commonly call the n-body problems.

If the two-body problem has been fully resolved, the one where the system has more than two bodies remains open. Many numerical approaches have flourished worldwide. The recent progress of computing tools and their power facilitated the research works of the different research teams to give an approximation of the behavior of each of bodies

*Corresponding author

of these systems. Let us go back in more detail to the history of such problems. But before that, by configuration, we mean the classic restricted problem of 3 bodies, the classic restricted 4 bodies problem in both triangular and collinear frames, the Hill problem, the Copenhagen problem, the Henon-Heiles problem, etc. By perturbations on one or more than one component of the system, we mean variable mass, resonance, drag force, solar radiation pressure, the shape of the bodies, modified Newton potential, Yukawa force, Yarkovasky force, asteroids belt effect, quantized correction, Coriolis and centrifugal forces, etc. Under one or more than one of the above perturbations, many research works have been published:
- For the classical restricted three-body problem, we can cite [1-9] - For the Hill problem, without being exhaustive, we can cite [10-16] - On the other hand, [17-22] studied the Robe problem, and [23-27] studied the Henon-Heiles system.
- Now for the restricted four-body problem under different perturbations as cited above, our principal citations are: [28-43]. Notice that for variable mass perturbation, until recently, the necessary adaptation of Newton' s second law to celestial systems, where some of their components have a variable mass, has not been taken into account. Noting that this variation in mass induces perceptible changes in the behaviour of the studied body, Plastino and Muzzio, in their article [44], attempted to remedy this. Nevertheless, before the publication of this work and during the recent decades, an important number of works on such systems have abounded here and there. Some took in account the perturbation in Newton's second law and some others considered that the effect on the system motion is negligible. However, we have also used, [45-57] to achieve the present work.

This paper is presented under several sections and sub-sections. The introduction is given in section 1. The equations of motion are determined in section 2. In section 3, we develop our numerical investigations. Section 4 is reserved to the stability states study of parking points. The conclusion is given in section 5.

2 Equations of motion

In this configuration, we consider four bodies of masses m_1, m_2, m_3, and m respectively, out of which the first three (the primaries) are assumed to be triaxial in shape, placed on the abscissa axis and the fourth body (the test particle) has a variable mass according to Jean's law. We also suppose that the test particle is moving in three dimensional space and it is subject to the effects of the primaries that it does not affect. We also assume that body of mass m_2 has a solar radiation effect with radiation parameter q and placed at the origin (see figure 1). Finally, we assume that the system is subject to the effects of Coriolis and centrifugal forces with respectively ϕ_1 and ϕ_2 as the forces parameters.

If $r = \xi.i + \eta.j + \zeta.k$, v and a are the position vector, velocity and acceleration of the test particle, then from the Newton's second law, the rate of change of momentum is an effective force F. i.e.

$$\frac{d(m\,v)}{d\,t} = F,$$
$$a + \frac{\dot{m}}{m}\,v = \frac{F}{m},$$
$$\ddot{r} + 2\,\phi_1\,(\omega \times \dot{r}) + \phi_2\,\omega \times (\omega \times r) + \frac{\dot{m}}{m}(\dot{r} + \phi_1.\omega \times r) = \frac{F}{m}.$$

Using the above definition and following the procedure given by [4], [51], and [58], the equations of motion of the variable mass test particle in the non-dimensional units can be

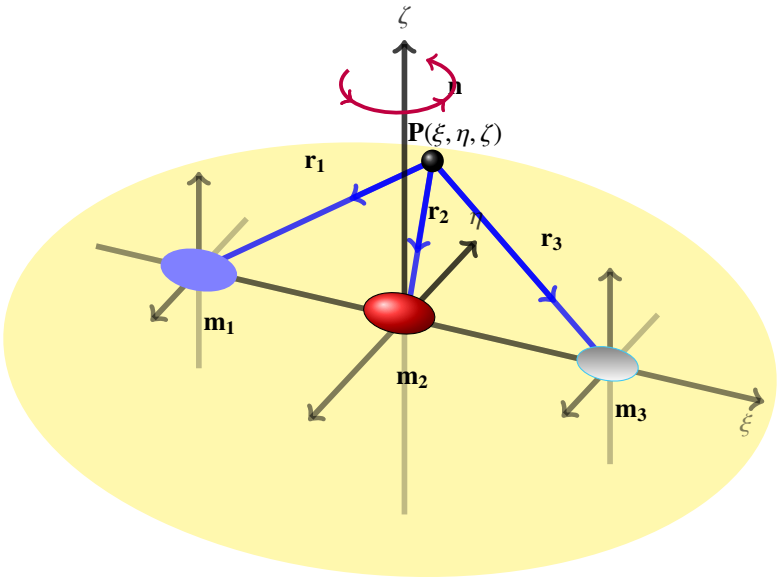

Figure 1: Geometric configuration of the problem with primaries as triaxial shapes

written as

$$\begin{cases} \ddot{\xi} - 2n\phi_1\dot{\eta} + \dfrac{\dot{m}}{m}(\dot{\xi} - n\phi_1\eta) = \dfrac{\partial P}{\partial \xi}, \\ \ddot{\eta} + 2n\phi_1\dot{\xi} + \dfrac{\dot{m}}{m}(\dot{\eta} + n\phi_1\xi) = \dfrac{\partial P}{\partial \eta}, \\ \ddot{\zeta} + \dfrac{\dot{m}}{m}\dot{\zeta} = \dfrac{\partial P}{\partial \zeta}, \end{cases} \tag{1}$$

where,

$$\begin{aligned} P = {} & \frac{n^2\phi_2}{2}(\xi^2+\eta^2) + \frac{1}{r_1}\left[1 + \frac{T_{11}}{2r_1^2} - \frac{3}{2r_1^4}(T_{21}\eta^2 + T_{31}\zeta^2)\right] \\ & + \frac{\mu q}{r_2}\left[1 + \frac{T_{12}}{2r_2^2} - \frac{3}{2r_2^4}(T_{22}\eta^2 + T_{32}\zeta^2)\right] + \frac{1}{r_3}\left[1 + \frac{T_{13}}{2r_3^2} - \frac{3}{2r_3^4}(T_{23}\eta^2 + T_{33}\zeta^2)\right], \\ r_i^2 = {} & (\xi - (i-2)/2)^2 + \eta^2 + \zeta^2, \\ n = {} & \sqrt{2(1+4\mu) + 3(T_{11}+T_{13}) + 48\mu(T_{11}+T_{12})}, \end{aligned}$$

and T_{ij}, $i, j = 1, 2, 3$, are the triaxiality parameters.

Du to the variable mass of the test particle, we will use Jeans Law [59]; $\dfrac{dm}{dt} = -\nu_1 m^S$, where ν_1 is a constant coefficient and $S = 1$ (notice that $0.4 \leq S \leq 4.4$). As Meshcherskii

space time transformation [60] is $(\xi, \eta, \zeta) = v_2^{-1/2}(x_1, y_1, z_1)$, we then get

$$\begin{cases} m = m_0\, e^{-v_1 t}, \\ (\dot{\xi}, \dot{\eta}, \dot{\zeta}) = v_2^{-1/2} \left\{ \dot{x}_1 + \dfrac{v_1}{2} x_1, \dot{y}_1 + \dfrac{v_1}{2} y_1, \dot{z}_1 + \dfrac{v_1}{2} z_1 \right\}, \\ (\ddot{\xi}, \ddot{\eta}, \ddot{\zeta}) = v_2^{-1/2} \left\{ \ddot{x}_1 + v_1 \dot{x}_1 + \dfrac{v_1^2}{4} x_1, \ddot{y}_1 + v_1\, \dot{y}_1 + \dfrac{v_1^2}{4} y_1, \ddot{z}_1 + v_1\, \dot{z}_1 + \dfrac{v_1^2}{4} z_1 \right\}, \end{cases} \tag{2}$$

where m_0 is the mass at time t = 0, and $v_2 = \dfrac{m}{m_0}$.
Using equations 1, and 2, the equations of motion become

$$\begin{cases} \ddot{x}_1 - 2\, n\, \phi_1\, \dot{y}_1 = \dfrac{\partial\, Q}{\partial\, x_1}, \\ \ddot{y}_1 + 2\, n\, \phi_1\, \dot{x}_1 = \dfrac{\partial\, Q}{\partial\, y_1}, \\ \ddot{z}_1 = \dfrac{\partial\, Q}{\partial\, z_1}, \end{cases} \tag{3}$$

where

$$\begin{aligned} Q = {} & \frac{n^2\, \phi_2}{2}(x_1^2 + y_1^2) + \frac{v_1^2}{8}(x_1^2 + y_1^2 + z_1^2) \\ & + v_2^{3/2}\Big[\frac{1}{\rho_1}\Big\{1 + \frac{T_{11}\, v_2}{2\rho_1^2} - \frac{3\, v_2}{2\rho_1^4}(T_{21}\, y_1^2 + T_{31}\, z_1^2)\Big\} + \frac{\mu\, q}{\rho_2}\Big\{1 + \frac{T_{12}\, v_2}{2\rho_2^2} - \frac{3\, v_2}{2\rho_2^4}(T_{22}\, y_1^2 + T_{32}\, z_1^2)\Big\} \\ & + \frac{1}{\rho_3}\Big\{1 + \frac{T_{13}\, v_2}{2\rho_3^2} - \frac{3\, v_2}{2\rho_3^4}(T_{23}\, y_1^2 + T_{33}\, z_1^2)\Big\}\Big], \\ \rho_1^2 = {} & (x_1 + v_2^{1/2})^2 + y_1^2 + z_1^2, \\ \rho_2^2 = {} & x_1^2 + y_1^2 + z_1^2, \\ \rho_3^2 = {} & (x_1 - v_2^{1/2})^2 + y_1^2 + z_1^2. \end{aligned}$$

From equation 3, the quasi-Jacobi integral can be written as

$$(\dot{x}_1^2 + \dot{y}_1^2 + \dot{z}_1^2) \;=\; 2\, Q + E + 2 \int_{t_0}^{t} \left(\frac{\partial Q}{\partial t} \right) dt, \tag{4}$$

where E is the quasi-Jacobi energy constant. $v_1 = 0$ and $v_2 = 1$, correspond to the system of constant mass.

3 Numerical Investigations

This section subdivided in many subsections, is devoted to locations of parking points, Poincaré surfaces, surfaces with projections and basins of attraction. For these investigations, the numerical values of the parameters are as follows

$\mu = 0.25$, $\phi_1 = \phi_2 = 1.2$, $T_{11} = 0.005$, $T_{21} = 0.0005$, $T_{31} = 0.00005$, $T_{12} = 0.002$, $T_{22} = 0.0002$, $T_{32} = 0.00002$, $T_{13} = 0.001$, $T_{23} = 0.0001$, $T_{33} = 0.00001$.

3.1 Locations of parking points

The parking points can be obtained by solving numerically the following system.

$$\begin{cases} \dfrac{\partial Q}{\partial x_1} = 0, \\ \dfrac{\partial Q}{\partial y_1} = 0, \\ \dfrac{\partial Q}{\partial z_1} = 0. \end{cases} \tag{5}$$

When we solve the first two equations by assuming $z_1 = 0$, we get the parking points in the $(x_1 - y_1)$-plane (i.e. the in-plane parking points). When we solve last two equations by assuming $x_1 = 0$, we get the parking points in the $(y_1 - z_1)$-plane (i.e. the out-of-plane parking points). For the out-of-plane parking points in the $(x_1 - z_1)$-plane are obtained when we solve the first and the last equations by assuming $y_1 = 0$. The Figures 2, 3, and 4, obtained numerically represent the location of the parking points in the above three cited planes.

Analyze of the obtained figures.

1. In Figure 2, there are six parking points out of which four are on the abscissa axis and two are on the ordinate axis. it can be also observed that as we increase the value of v_2, all the six parking points move away from the origin.

2. The sub-figures of Figure 3, correspond to two cases; constant mass case (a) and variable mass case (b). In the constant mass case, there are only two parking points that appear on the y_1-axis while in the variable mass case, there are two more parking points that appear on the z_1-axis.

3. Similarly, the sub-figures of Figure 4 show that in the constant mass case, there are four parking points on the x_1-axis and two additional parking points on the z_1-axis in the variable mass case.
   It can be concluded that the variable mass factor generates two new parking points in the out-of-plane.

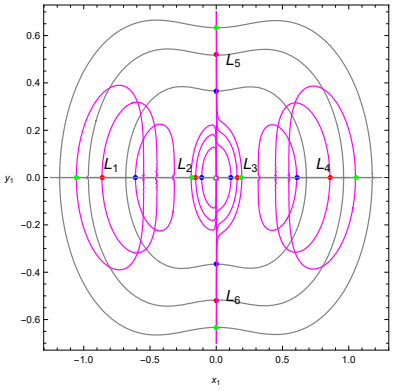

Figure 2: Locations of parking points in $x_1 - y_1-$plane at $v_1 = 0.2$ and $v_2 = 0.4$ (blue), 0.8 (red), 1.2 (green).

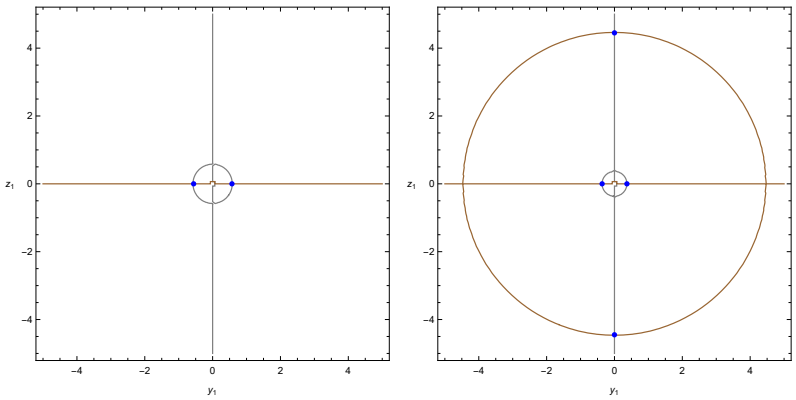

(a) At $v_1 = 0$ and $v_2 = 1$ (b) At $v_1 = 0.2$ and $v_2 = 0.4$

Figure 3: Locations of parking points in $y_1 - z_1$–plane.

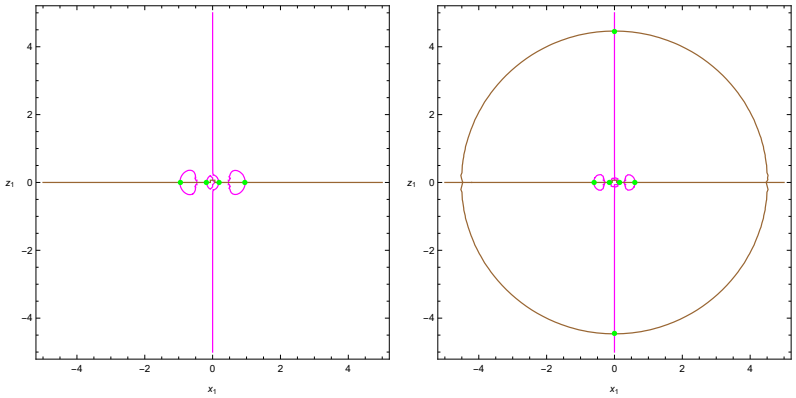

(a) At $v_1 = 0$ and $v_2 = 1$ (b) At $v_1 = 0.2$ and $v_2 = 0.4$

Figure 4: Locations of parking points in $x_1 - z_1$–plane.

3.2 Poincaré surfaces of section

Poincaré surfaces of section is one of the most important dynamical properties of the motion of the particle and from where we can detect the chaos. We start by writing equations of motion in the phase plane and then we graph these surfaces using Mathematica. The sub-figures of Figure 5, illustrate these surfaces in the $x_1 - \dot{x}_1$-plane and the $y_1 - \dot{y}_1$-plane respectively for two values of the parameters (v_1, v_2).

3.3 Surfaces with projections

To illustrate the surfaces with projection, we will follow the procedure given by [61]. The projections of the surfaces onto the configuration plane are known as Hills regions. The boundaries of these regions are the zero-velocity curves, the locus in the configuration plane and correspond to zero kinetic energy. We have plotted these surfaces with projections corresponding to the parking points in the $(x_1 - y_1)$–plane and given in Figure 6. Similarly, we can plot the surfaces in out-of-plane.

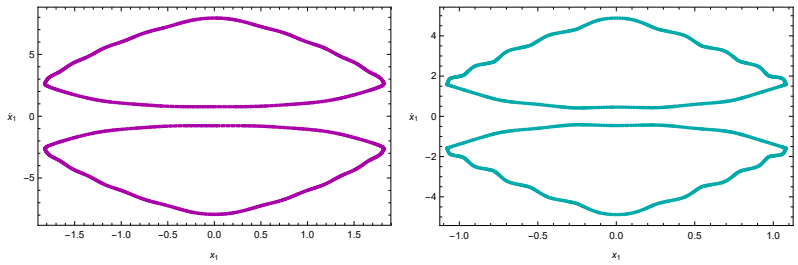

(a) For $v_1 = 0$ and $v_2 = 1$ (b) For $v_1 = 0.2$ and $v_2 = 0.4$

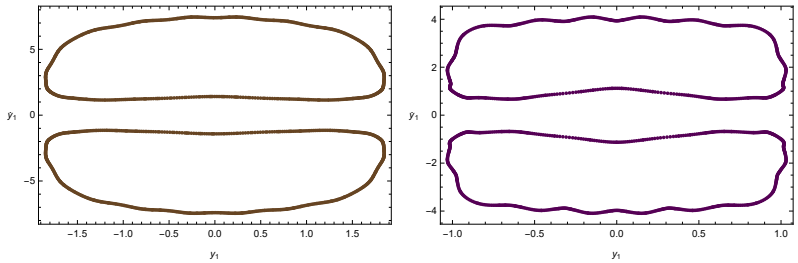

(c) For $v_1 = 0$ and $v_2 = 1$ (d) For $v_1 = 0.2$ and $v_2 = 0.4$

Figure 5: Poincaré surfaces of section.

3.4 Basins of convergence

As the above characteristics, the basins of convergence is also one of the most important dynamical properties of the motion of the test particle. We illustrated them by using the N-R method in the $(x_1 - y_1)$-plane. These basins are the composition of all initial conditions that converge to parking points. The iterative code to study this property is as follows

$$\begin{cases} x_{1_{n+1}} = x_{1_n} - \dfrac{Q_{x_1} Q_{y_1 y_1} - Q_{y_1} Q_{x_1 y_1}}{Q_{x_1 x_1} Q_{y_1 y_1} - Q_{x_1 y_1} Q_{y_1 x_1}}, \\ y_{1_{n+1}} = y_{1_n} - \dfrac{Q_{y_1} Q_{x_1 x_1} - Q_{x_1} Q_{x_1 y_1}}{Q_{x_1 x_1} Q_{y_1 y_1} - Q_{x_1 y_1} Q_{y_1 x_1}}, \end{cases} \tag{6}$$

where x_{1_n} and y_{1_n} are the values of n^{th} step for x_1 and y_1 in the N-R iterative process. (x_1, y_1) will be in the basins if the initial point converges rapidly to one of the parking points. If it converges to an attractor (parking point) then the process will stop and basins will be generated. We classify parking points on the plane by color code.

The Sub-Figure 7(a) shows the basins of attraction in the $(x_1 - y_1)$-plane, while the Sub-Figure 7(b) represents the zoomed part of the attracting domain near the attracting points. The attracting points $L_i, (i = 1, \ldots, 4)$ lie in the cyan color region while the attracting points $L_i, (i = 5, 6)$ lie in the blue and green color regions respectively. Notice that these regions extend to infinity.

Similarly, we can illustrate the basins of attraction in the out-of-plane.

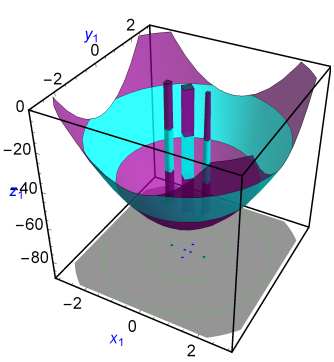

(a) Corresponding to L_1

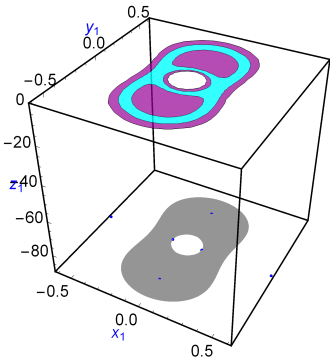

(b) Corresponding to $L_{2,3}$

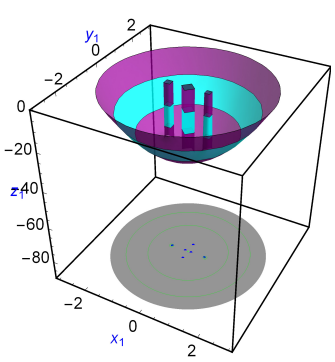

(c) Corresponding to L_4

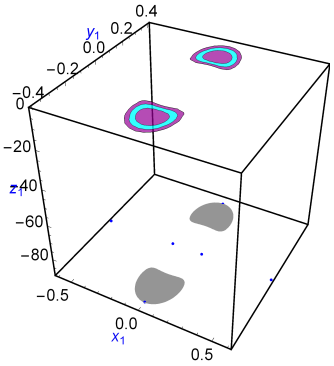

(d) Corresponding to $L_{5,6}$

Figure 6: Surfaces with projections

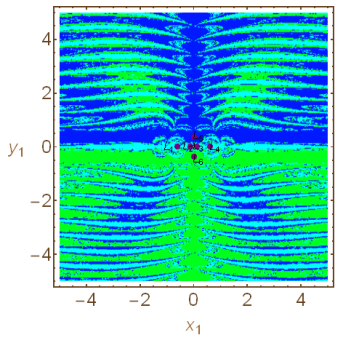

(a) For $v_1 = 0.2$ and $v_2 = 0.4$

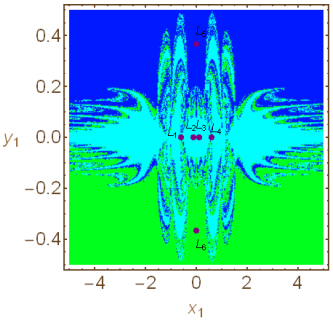

(b) Zoomed part of figure (a) near parking points

Figure 7: Basins of attractions

4 Stability states

To study the stability, we will follow the procedures as in [60], and in [54] The characteristic polynomial of equation 3 will then be

$$\lambda^6 + H_5\ \lambda^5 + H_4\ \lambda^4 + H_3\ \lambda^3 + H_2\ \lambda^2 + H_1\ \lambda + H_0 = 0, \tag{7}$$

where

$$\begin{aligned}
H_5 &= -3v_1,\\
H_4 &= 4\,\phi_1^2\,n^2 \;-\; Q^0_{x_1x_1} \;-\; Q^0_{y_1y_1} \;-\; Q^0_{z_1z_1} \;+\; \frac{15}{4}\,v_1^2,\\
H_3 &= 2\,v_1\,(Q^0_{x_1x_1} \;+\; Q^0_{y_1y_1} \;+\; Q^0_{z_1z_1} \;-\; \frac{5}{4}\,v_1^2 \;-\; 4\,\phi_1^2\,n^2),\\
H_2 &= \frac{15}{16}\,v_1^4 \;+\; \frac{3}{2}\,v_1^2\,(4\,\phi_1^2\,n^2 \;-\; Q^0_{x_1x_1} \;-\; Q^0_{y_1y_1} \;-\; Q^0_{z_1z_1})\\
&\quad -\;[\,\{4\,\phi_1^2\,n^2 \;-\; Q^0_{x_1x_1} \;-\; Q^0_{y_1y_1}\}\,Q^0_{z_1z_1}\\
&\quad +\;(Q^0_{x_1y_1})^2 \;+\; (Q^0_{x_1z_1})^2 \;+\; (Q^0_{y_1z_1})^2 \;-\; Q^0_{x_1x_1}\,Q^0_{y_1y_1}\,],\\
H_1 &= -\,\frac{3}{16}\,v_1^5 \;+\; \frac{v_1^3}{2}\{\,Q^0_{x_1x_1} \;+\; Q^0_{y_1y_1} \;+\; Q^0_{z_1z_1} \;-\; 4\,\phi_1^2\,n^2\}\\
&\quad +\;v_1\,[(Q^0_{x_1y_1})^2 \;+\; (Q^0_{x_1z_1})^2 \;+\; (Q^0_{y_1z_1})^2 \;-\; Q^0_{x_1x_1}\;Q^0_{y_1y_1}\\
&\quad +\;\{\,4\,\phi_1^2\,n^2 \;-\; Q^0_{x_1x_1} \;-\; Q^0_{y_1y_1}\,\}\,Q^0_{z_1z_1}\,],\\
H_0 &= \frac{1}{64}\,v_1^6 \;+\; \frac{1}{16}\,v_1^4\{4\,\phi_1^2\,n^2 \;-\; Q^0_{x_1x_1} \;-\; Q^0_{y_1y_1} \;-\; Q^0_{z_1z_1}\}\\
&\quad -\;\frac{1}{4}\,v_1^2\,[\{4\,\phi_1^2\,n^2 \;-\; Q^0_{x_1x_1} \;-\; Q^0_{y_1y_1}\}\,Q^0_{z_1z_1} \;+\; (Q^0_{x_1y_1})^2 \;+\; (Q^0_{x_1z_1})^2\\
&\quad +\;(Q^0_{y_1z_1})^2 \;-\; Q^0_{x_1x_1}\;Q^0_{y_1y_1}\,] \;+\; (Q^0_{x_1z_1})^2\,Q^0_{y_1y_1} \;+\; Q^0_{x_1x_1}\,(Q^0_{y_1z_1})^2\\
&\quad +\;(Q^0_{x_1y_1})^2\,Q^0_{z_1z_1} \;-\; Q^0_{x_1x_1}\,Q^0_{y_1y_1}\,Q^0_{z_1z_1} \;-\; Q^0_{x_1y_1}\,Q^0_{x_1z_1}\,Q^0_{y_1z_1}\\
&\quad +\;(Q^0_{x_1y_1})^2\,Q^0_{z_1z_1} \;-\; Q^0_{x_1x_1}\,Q^0_{y_1y_1}\,Q^0_{z_1z_1} \;-\; Q^0_{x_1y_1}\,Q^0_{x_1z_1}\,Q^0_{y_1z_1}\,.
\end{aligned}$$

The numerical solutions of equation 7 are given in the following tables and they correspond to the parking points. From these collected values, we observed that all the roots are either a positive real number or a complex number with positive real part. All the parking points either in-plane or out-of-plane are then unstable.

5 Conclusion

The mass variation effect is studied in the collinear restricted 4-body configuration where three primary bodies are taken as triaxial in shapes and placed in the consecutive order on the abscissa axis. Out of these three triaxial bodies the middle one is taken as source of radiation pressure. We also assume that the system is perturbed by Coriolis and centrifugal forces. From the obtained equations of motion, we evaluated six parking points in the in-plane motion and four parking points in the out-of-plane motion. In the classical case, there are six parking points in the in-plane motion and two parking points in the out-of-plane motion. We have illustrated the Poincaré surfaces of section and found that the surfaces are symmetrical about the abscissa axis. The system doesn't present any chaos. Further, the surfaces with projections are performed corresponding to each parking point. For the basins

Table 1: The nature of in-plane parking points at $v_1 = 0.2$, $v_2 = 0.4$, and $\phi_1 = \phi_2 = 1.4$.

Parking Point		Roots	Nature
$x_1 - Co.$	$y_1 - Co.$		
± 0.6100000000	0.0000000000	$0.09999999999 - 426.7597201310\,i$ $0.0999999999 + 132.0000000000\,i$ $0.1000000000 \pm 398.0676917576\,i$ ± 762.2185412135	Unstable
± 0.1100000000	0.0000000000	$0.0999999999 \pm 7.4539857542\,i$ $0.1000000007 \pm 7.2187591245\,i$ -9.9957585811 10.1957585811	Unstable
0.0000000000	± 0.3650000000	$-0.4286698320 \pm 2.4237724816\,i$ $0.0999999999 \pm 1.5920864564\,i$ $0.6286698320 \pm 2.4237724816\,i$	Unstable

Table 2: The nature of out-of-plane parking points at $v_1 = 0.2$, $v_2 = 0.4$, $x_1 = 0$, and $\phi_1 = \phi_2 = 1.4$.

Parking Point		Roots	Nature
$y_1 - Co.$	$z_1 - Co.$		
± 0.3650000000	0.0000000000	$0.0999999984 \pm 1.5840228164\,i$ $0.0999999996 \pm 3.8511170670\,i$ $0.1000000023 \pm 1.8101983636\,i$	Unstable
0.0000000000	± 4.4500000000	$0.0999999999 \pm 4.3498097428\,i$ $0.1000000003 \pm 1.3211407943\,i$ -0.0489253328 0.2489253328	Unstable

Table 3: The nature of out-of-plane parking points at $v_1 = 0.2$, $v_2 = 0.4$, $y_1 = 0$, and $\phi_1 = \phi_2 = 1.4$.

Parking Point		Roots	Nature
$x_1 - Co.$	$z_1 - Co.$		
0.0000000000	± 4.4500000000	$0.1000000000 \pm 4.3498097428\,i$ $0.1000000003 \pm 1.3211407943\,i$ -0.0489253328 0.2489253328	Unstable

of attraction corresponding to the attracting points, one of the most important dynamical properties of the motion, they extended to infinity. Finally, the stability of the parking points turned out to be unstable in this configuration.

Acknowledgment

The first author is thankful to the International Center for Advanced Interdisciplinary Research (ICAIR), New Delhi, India for providing the research facilities for this research paper. We are also grateful to reviewers for their comments that made the paper more readable.

Authors' Contributions

All authors have the same contribution.

Data Availability

No data available.

Conflicts of Interest

The authors declare that there is no conflict of interest.

Ethical Considerations

The authors have diligently addressed ethical concerns, such as informed consent, plagiarism, data fabrication, misconduct, falsification, double publication, redundancy, submission, and other related matters.

Funding

This research did not receive any grant from funding agencies in the public, commercial, or nonprofit sectors.

References

[1] Abdulraheem, A., Singh, J. 2008, Astrophys. Space Sci., 317, 9.

[2] Bhatnagar, K. B., Hallan, P. P. 1979, Celest. Mech., 18, 105.

[3] Bhatnagar, K. B., Hallan, P. P. 1995, Celest. Mech., 20, 95.

[4] Sharma, K. R., Taqvi, Z. A., Bhatnagar, K. B. 2001, Celest. Mech. Dyn. Astro., 79, 119.

[5] Abozaid, A. A., Selim, H. H., Gadallah, K. A. K., Hassan, I. A., Abouelmagd, E. I. 2020, Applied Mathematics and Nonlinear Sciences, 5, 157.

[6] Abouelmagd, E. I., García Guirao, J. L., Pal, A. K. 2020a, New Astronomy, 75, 101319.

[7] Alshaery, A. A., Abouelmagd, E. I. 2020, Results in Physics, 17, 103067.

[8] Ansari, A. A. 2021a, Bulgarian Astronomical Journal, 35.

[9] Ansari, A. A., Alam, M., Meena, K. R., Ali, A. 2021, Appl. Math. Inf. Sci., 15, 189.

[10] Scheeres, D. 1998, Celest. Mech. Dyn. Astro., 70, 75.

[11] Scheeres, D. J., Bellerose, J. 2005, Dynamical Systems: An International Journal, 20, 23.

[12] Ansari, A. A. 2021b, Astronomy reports, 65, 1179.

[13] Markellos, V. V., Roy, A. E. 1981, Celest. Mech., 32, 269.

[14] Markellos, V. V., Roy, A. E., Velgakis, M. J., Kanavos, S. S. 2000, Astrophys. Space Sci., 271, 293.

[15] Markellos, V. V., Roy, A. E., Perdios, E. A., Douskos, C. N. 2001, Astrophys. Space Sci., 278, 295.

[16] Douskos, C. N. 2010, Astrophys. Space Sci., 326, 263.

[17] Robe, H. A. G. 1978, Celest. Mech., 16, 343.

[18] Hallan, P. P., Mangang, K. B. 2007, Indian Journal of pure and applied Mathematics, 38, 17.

[19] Singh, J., Mohammed, H. L. 2012, Earth, Moon, Planets, 109, 1.

[20] Ansari, A. A., Singh, J., Alhussain, Z., Belmabrouk, H. 2019, New Astronomy, 73, 101280.

[21] Ansari, A. A. 2020, New Astronomy, 83.

[22] Abouelmagd, E. I., Ansari, A. A., Shehata, S. H. 2020b, Inter. J. Geom. Meth. in Modern Physics, 18, 2150005.

[23] Hanon, M., Heiles, C. 1964, The astronomical journal, 69, 73.

[24] Aguirre, J., Vallejo, J. C., Sanjuan, M. A. F. 2001, Physical Review E, 64, 066208.

[25] Ansari, A. A., Abouelmagd, A. E. 2021, Modern Physics Letters A, 36.

[26] Abouelmagd, E. I., Ansari, A. A. 2022, Astronomy reports, 66, 64.

[27] Sahdev, S. K., Ansari, A. A. 2022, Applications and Applied Mathematics: An Int. J., 17, 439.

[28] Bhatnagar, K. B. 1970, Indian J. of Pure and Applied Math., 2, 583.

[29] Michalodimitrakis, M. 1981, Astrophys. Space Sci., 75, 289.

[30] Maranhao, D., Llibre, J. 1998, Celest. Mech. Dyn. Astro., 71, 1.

[31] Leandro, E. 2006, J. Differential Equations, 226, 323.

[32] Papadakis, K. 2007, Planet. Space Sci., 55, 1368.

[33] Kalvouridis, T. J., Arribas, M., Elipe, A. 2007, Planet. Space Sci., 55, 475.

[34] Baltagiannis, A. N., Papadakis, K. E. 2011, Int. J. Bifurc. Chaos, 21, 2179.

[35] Papadouris, J., Papadakis, K. 2013, Astrophys. Space Sci., 344, 21.

[36] Kumari, R., Kushvah, B. S. 2014, Astrophy. Space Sci., 349, 693.

[37] Ansari, A.A. 2014, Invertis Journal of Science and Technology, 7, 29.

[38] Arribas, M., Abad, A., Elipe, A., Palacios, M. 2016a, Astrophys. Space Sci., 361.

[39] Arribas, M. Abad, A. Elipe, A., Palacios, M. 2016b, Astrophys. Space Sci., 361.

[40] Singh, J., Vincent, A. 2016, Few-Body Syst., 57, 83.

[41] Palacios, M., Arribas, M., Abad, A., Elipe, A. 2019, Celest. Mech., 131, 16.

[42] Ansari, A. A., Prasad, S. N. 2020, Astron. Lett., 46, 275.

[43] Llibre, J., Pasca, D., Valls, C. 2021, Celestial Mech. Dyn. Astr., 133.

[44] Plastino, A.R., Musio, J.C. 1992, Celestial Mech. Dyn. Astr., 53, 227.

[45] Hadjidemetriou, J. 1963, Icarus, 2, 440.

[46] Hadjidemetriou, J. 1967, Adv. Astron. Astrophys., 5, 131.

[47] Singh, J., Ishwar, B. 1985, Celest. Mech., 35, 201.

[48] Adler, C. 1987, Am. J. Phys., 55, 739.

[49] Lukyanov, L. G. 2009, Astron. Lett., 35, 349.

[50] Zhang, M. J., Zhao, C. Y., Xiong, Y. Q. 2012, Astrophys. Space Sci., 337, 107.

[51] Abouelmagd, E. I., Mostafa, A. 2015, Astrophys. Space Sci., 357.

[52] Ansari, A. A. 2017, Italian Journal Of Pure and Applied Mathematics, 38, 581.

[53] Ansari, A. A., Meena, K. R., Prasad, S. N. 2020, Romanian Astron. J., 30, 135.

[54] Bouaziz, F., Ansari, A.A. 2021, Astron. Nachr., 342, 666.

[55] Albidah, A. B., Ansari, A. A. 2023, Astronomy reports.

[56] Albidah, A. B., Ansari, A.A., Kellil, R. 2023, Astronomy and computing, 42.

[57] Abdullah, Ali, M. 2024, to appear in Solar System Research.

[58] Ansari, A. A., Sahdev, S. K. 2022, Astronomy reports, 66, 1074.

[59] Jeans, J. H. 1928, Astronomy and Cosmogony, Cambridge University Press, Cambridge.

[60] Meshcherskii,I. V. 1949, Works on the mechanics of bodies of variable mass, GITTL, Moscow.

[61] Kellil, F. B. 2021, Astronomy letters, 47.